Composite Structures 159 (2017) 761–772

Contents lists available at ScienceDirect

Composite Structures

journal homepage: www.elsevier.com/locate/compstruct

Mechanical, thermal and interfacial performances of carbon fiber reinforced composites flavored by carbon nanotube in matrix/interface

Zhongbo Zhao [1], Kunyue Teng [1], Nan Li, Xiaojie Li, Zhiwei Xu *, Lei Chen, Jiarong Niu, Hongjun Fu, Lihuan Zhao, Ya Liu

Key Laboratory of Advanced Braided Composites, Ministry of Education, School of Textiles, Tianjin Polytechnic University, Tianjin 300387, China

ARTICLE INFO

Article history:
Received 3 August 2016
Revised 20 September 2016
Accepted 8 October 2016
Available online 11 October 2016

Keywords:
Carbon nanotubes
Energy dispersive X-ray spectroscopy
Interfacial shear strength
Gradient interface layer

ABSTRACT

The introduction of carbon nanotubes (CNTs) into fiber-reinforced polymer composites has been achieved predominantly via two routes: mixing CNTs entirely throughout the matrix (matrix modification) or attaching CNTs onto reinforcing fibers (interface modification). We studied unidirectional carbon fiber/epoxy composites where CNTs were introduced to enhance the hierarchical composites by two alternative strategies: mixing into the epoxy or attaching onto carbon fibers by electrophoretic deposition. Single-fiber fragmentation test combined with energy dispersive X-ray spectroscopy was creatively applied to calculate interfacial shear strength and improvements of 45.2% and 10.14% were achieved for hierarchical composites based on CNT-modified fibers (CF-CNTs/EP) and composites based on CNT-reinforced matrix (CF/EP-CNTs), respectively. Increases of 24.42% for CF-CNTs/EP and 10.41% for CF/EP-CNTs in tensile strength were achieved separately. The superiorities of CF-CNTs/EP were derived from that gradient interface layer formed due to the introduction of CNTs in interface and it was not obvious in CF/EP-CNTs.

1. Introduction

Carbon fiber-reinforced polymer composites with chemical and environmental resistance have superior strength-to-weight and stiffness-to-weight ratios, which make them ideal for many structural applications in many fields, such as aerospace, automotive, sports equipment and so on. The properties of fiber-reinforced polymer composites are, to a great extent, controlled by the performance of the interface which works as a bridge between fiber and matrix. Preeminent interfacial bonding ensures efficient load transfer from matrix to the fibers and internal crack propagation, which helps reduce stress concentrations and improve the ultimate performance of composites [1–3]. Due to their unique structures, excellent mechanical properties where the strength, modulus and resilience are equal or superior to any current materials, brilliant electrical and thermal properties, carbon nanotubes (CNTs) have been employed to enhance the hierarchical composites, which is a topic of significant interest in recent years [4,5].

Carbon fibers (CFs) show crystallized graphitic basal planes with non-polar surface and the chemical inertness due to the high temperature carbonization/graphitization step during manufacturing process [6]. Excessive smoothness and few polar groups of CFs lead to weak bondings with matrices [7,8]. According to the characteristics of CFs, the introduction of CNTs into carbon fiber-reinforced polymer composites has been attained, which was fundamentally based on two techniques: mixing CNTs entirely throughout the matrix (matrix modification) or attaching CNTs directly onto fiber surface (interface modification) (Fig. 1.). To date, direct mixing by mechanical [9], shear mixing involving a three-roll mill [10,11], or ultrasonic techniques was generally used to mix CNTs into low-viscosity thermosetting matrices. And, generally, five techniques to graft or attach CNTs onto carbon fiber surface have been reported so far: (1) direct growth of CNTs on fibers by chemical vapor deposition (CVD) [12–14]; (2) chemical reactions between functionalized CNTs and fibers [3,15,16]; (3) electrophoretic deposition (EPD) of CNTs on fiber surface [17]; (4) coating of fibers with CNT-containing sizing [2,18,19]; (5) immersing fibers in the solution of CNTs [19].

The most simple and straightforward manufacturing process for introduction of CNTs involves matrix modification, i.e. direct mixing CNTs into the matrix. Functionalized CNTs, treated by either chemical or physical treatments, can make a favor for promoting the CNT dispersion and stress transferring between CNTs and matrices. Matrix modification commonly has the advantages of

* Corresponding author.
E-mail address: xuzhiwei@tjpu.edu.cn (Z. Xu).
[1] These authors contributed equally to this work.

http://dx.doi.org/10.1016/j.compstruct.2016.10.022
0263-8223/

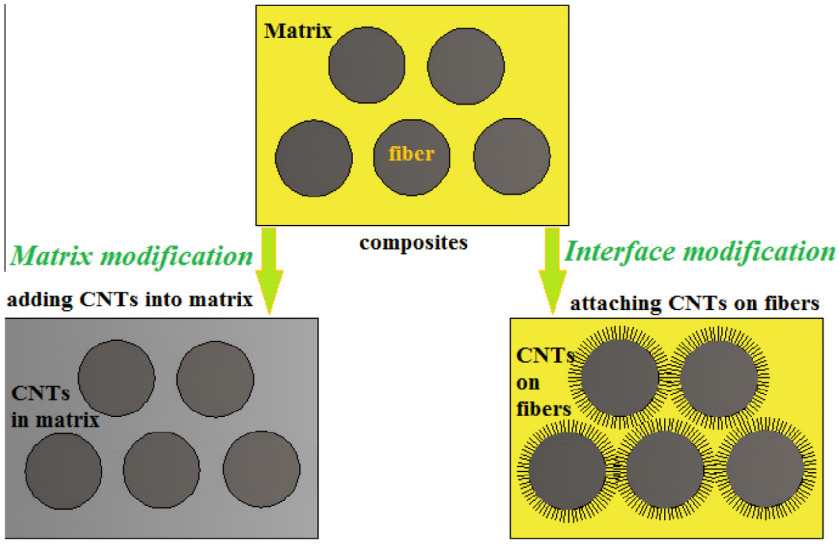

Fig. 1. Schematic diagrams of fiber-reinforced polymer composites and CNT-based hierarchical polymer composites.

simplicity and compatibility with standard industrial techniques. This technique has been applied by a number of commercial companies and a variety of CNT-modified matrix products are now commercially available. Grafting CNTs onto fiber surfaces with proverbial superiority, efficaciously, could acquire higher loadings of CNTs with a radial orientation [20], which is expected to be optimal for transverse reinforcement [5,21]. Researchers [3,15,16,22] have applied chemical methods to covalently graft functionalized CNTs onto functionalized CFs. Thostenson [12] firstly synthesized CNTs via thermal chemical vapor deposition on the surfaces of CFs. Bekyarova et al. [17] authenticated that a uniform distribution of CNTs on the surface of carbon fabric could be obtained using EPD technique, in which both as-received and oxygenated CNTs were deposited onto CFs. EPD technology has the advantages of simplification and uniform deposition which could be applied to continuous processing of carbon fiber tows. Alternatively, CNTs have been attached onto CFs by using a nanocomposite polymer sizing [18,23,24]. Repetitious sizing treatment was used to modify the carbon fiber surfaces with CNTs for improving interfacial properties of CF/epoxy composites [19].

However, up to present, few systematic investigations and comparisons of matrix modification and interface modification have been reported. So, in this work, we focused on two alternative ways to introduce CNTs to composites: mixing CNTs in the matrix using ultrasonic technique (matrix modification) or depositing on carbon fiber surface using EPD technology (interface modification); meanwhile strength and weakness of the two alternative strategies were contrasted. Morphologies of carbon fiber surface and fracture structures obtained from mechanical tests were characterized by scanning electron microscopy (SEM). Moreover, the distribution of CNTs on carbon fiber surface and in matrix was detected by transmission electron microscope (TEM). Common mechanical tests, including flexural test and tensile strength test, were carried out. Simultaneously, the thermal properties of the neat epoxy (EP) and hierarchical composites were characterized by dynamic mechanical thermal analysis (DMA). In addition, the interlaminar shear strength (ILSS) and interfacial shear strength (IFSS) which indicate the interfacial properties of hierarchical composites were also investigated, respectively, using short beam shear test and single-fiber fragmentation test. For matrix modification, the presence of CNTs in the resin led to the opaque of matrix (Fig. S1). Therefore, during single-fiber fragmentation test, fragments and birefringence phenomenon cannot be caught and the IFSS was unable to be measured. We made great efforts to conquer this problem and adopted energy dispersive X-ray spectroscopy (EDS) equipped on SEM to assist single-fiber fragmentation test. Finally, EDS, force modulation atomic force microscope (f-AFM) and TEM techniques were used to survey the microstructures of interface and explore the enhancement mechanism of CNTs.

2. Materials and experimental methods

2.1. Materials

Commercially-available T700S CFs (Toray) with the diameter of 7 μm were employed in this study. As-received multi-wall CNTs (Chengdu Organic Chemicals Co. Ltd., Chinese Academy of Sciences) with a diameter of 30–50 nm, length of 10–20 μm and purity of more than 95wt% were adopted in this study. JC-02A modified epoxy and JH-0511 modified 2-ethyl-4-methylimidazole, used as accelerant, were purchased from Changshu Jia Fa Chemical Co. Ltd., China. We selected tetrahydrophthalic anhydride as the curing agent.

2.2. Introduction of CNTs onto carbon fiber surface and into matrix

In order to better appraise the influences of CNTs on the modification of composites, virgin CFs were refluxed by acetone in the soxhlet apparatus at 70 °C for 48 h to remove the commercial sizing. Subsequently, CFs were dried 3 h under vacuum at 50 °C and the unsized CFs were also designated with CFs. And CFs were on behalf of unsized CFs in the following statements, if there is no special note. As-received CNTs were treated with a mixture of concentrated sulfuric acid (H_2SO_4)/concentrated nitric acid (HNO_3) (3:1 v/v) to introduce carboxylic acid groups (-COOH) to CNTs [25]. Similarly, the abbreviation of CNTs stands for functionalized CNTs in the following descriptions.

2.2.1. Electrophoretic deposition of CNTs onto carbon fiber surface

Referring to references [26–30] and our previous research [19], we chose these EPD parameters: concentration of CNTs 0.3 mg/ml, deposition voltage 24V, deposition time 5 min, electrode materials metal plate and electrode separation 50 mm. 300 mg CNTs containing carboxyl groups were initially dispersed in 1000 ml of deionized water by an ultrasonic bath for 2 h to achieve a homogenous suspension. After that, the unsized carbon fiber tow was immersed into the suspension, and a succedent process of EPD was shown in Fig. 2(a).

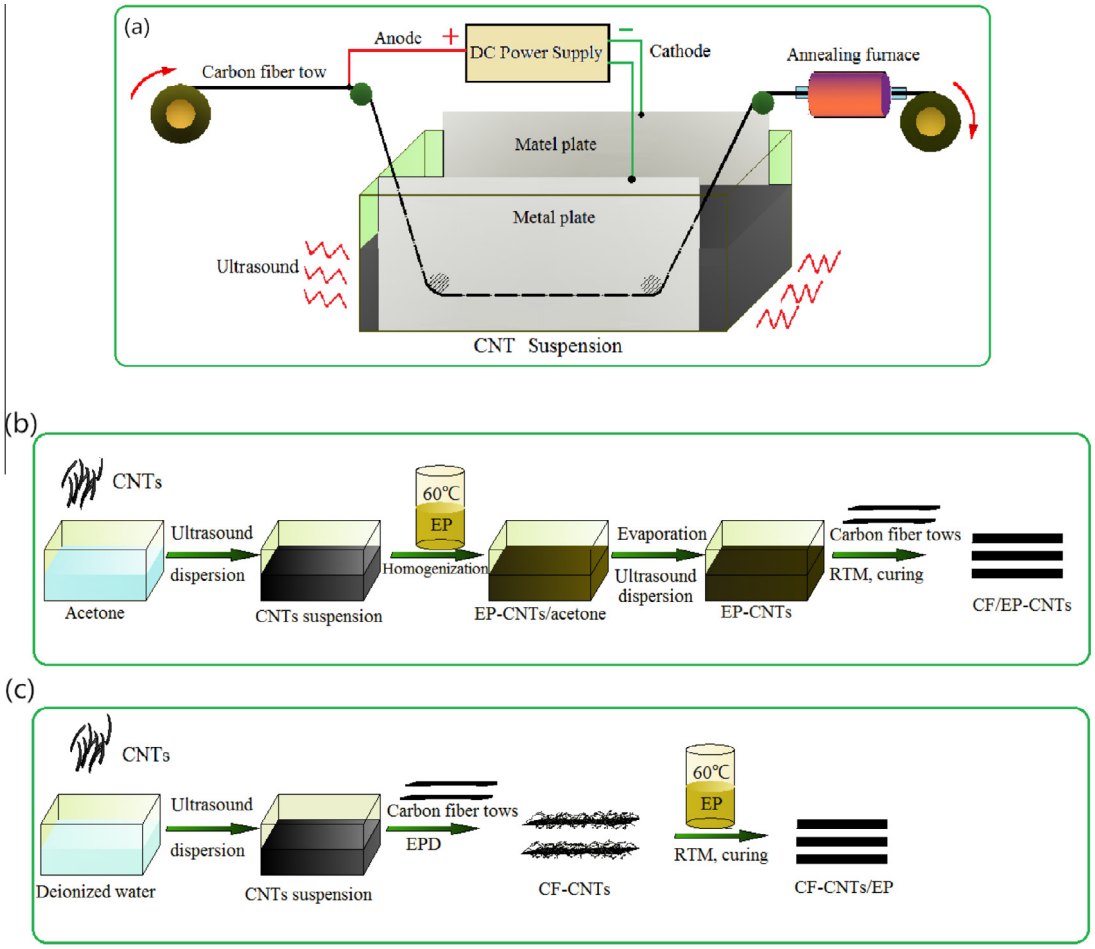

Fig. 2. Diagrammatic sketch of the EPD procedure (a); flowchart for the fabrication process of (b) CF/EP-CNTs, (c) CF-CNTs/EP.

It is necessary to explain that the carbon fiber tow was not continuously passed through the suspension. Every five minutes and a half, there was 25 cm carbon fiber tow that passed through the suspension. Before the direct-current power was switched on, to disperse the carbon fiber tow, fiber tow was treated by ultrasonic for 30 s which could make CNTs enter carbon fiber tow when the voltage was loaded onto the carbon fiber tow. The weight ratio of CNTs was 0.15 wt% after electrophoretic deposition. CNTs functionalized CFs obtained in this step were named as deposited CFs and designated with CF-CNTs.

2.2.2. Mixing CNTs into the matrix

Firstly, CNTs were dispersed in acetone by an ultrasonic bath for 2 h to achieve a uniform suspension. The suspension was mixed with the matrix which was mixed by epoxy resin, harder and accelerant well in a weight ratio of 100:70:1, subsequently the mixture was dispersed by ultrasonic until all acetone volatilized and the mixing progress was shown in Fig. 2(b). The CNTs were dispersed in the matrix at a concentration of 0.35 wt% which was equivalent to EPD progress when the hierarchical composites were completed. This sample was named as CNTs functionalized matrix and designated with EP-CNTs.

2.3. Production of composite samples

2.3.1. Production of unidirectional composite samples

The flowchart for the fabrication process was shown in Fig. 2(b) and (c). Firstly, fiber tows were placed along the axis into the groove of the mold and the fiber-volume fraction of ultima composites was about 45%. Secondly, the prepared matrix was infused with resin transfer molding technique under a pressure of 0.1 MPa. Subsequently, the mold was put into an oven and composites were cured by a curing step at 90 °C for 3 h, 120 °C for 3 h and 150 °C for 5 h and the final dimension of samples was 220 mm × 10 mm × 2 mm. The composites obtained in this step were named as CF/EP (carbon fiber reinforced EP composites), CF/EP-CNTs (hierarchical composites based on CNT-reinforced matrix), and CF-CNTs/EP (hierarchical composites based on CNT-modified fibers) respectively.

2.3.2. Production of single-fiber fragmentation specimens

Firstly, single fiber was separated from carbon fiber bundle carefully. The single fiber, then, was placed into the midst of the dumbbell shaped groove of the mold. Necessarily, heat-resistant adhesive tape was used to hold the fiber ends with pieces of cardboard, in order to make single fibers straight in the samples. Subsequently, the mixed epoxy resin was added into the mold. Samples were removed from the mold, carefully, after the specimen had cured and cooled to room temperature. The final gauge dimensions (unit: mm) were shown in Fig. 3(a); all samples were lightly sanded to remove burs and edge irregularity.

2.4. Characterizations

2.4.1. Characterizations of CFs

Surface morphologies of CFs were characterized by SEM (Hitachi S-4800, Japan) and single-fiber tensile strength test was carried for Weibull analysis. Moreover, the distribution of CNTs

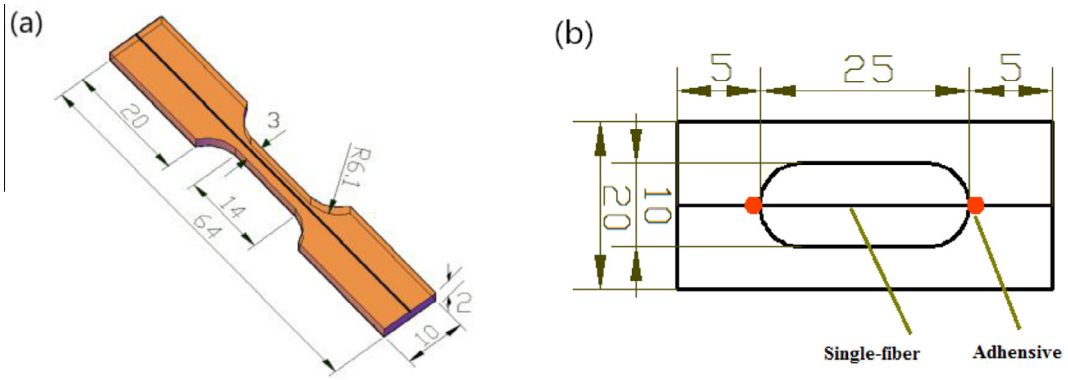

Fig. 3. Dimensional drawing of single-fiber fragmentation specimens (a) and single-filament test specimen (b).

on carbon fiber surface was detected by SEM and TEM. Single-fiber tensile strength test was performed at a crosshead speed of 2 mm/s at room temperature. The fiber was fixed at a thin sheet of paper, with slot of length 25 ± 0.5 mm, as shown in Fig. 3(b). A minimum of twenty measurements were prepared for each fiber specimen. The fiber diameter was determined using SEM and averaging at least five measurements per fiber.

2.4.2. Characterizations of composites

According to the standards JC/T773-2010, ASTM D790-03 and GB/T 1447-2005, the short beam shear tests, from which we can evaluate interlaminar shear strength, flexural tests and tensile strength tests were carried out on a universal testing machine (Instron 3369, USA). At least five specimens for each composite condition were tested to obtain average value and all tests were carried out at room temperature. Dynamic mechanical thermal analysis could characterize the viscoelastic properties of the materials and was used to determine storage modulus (E′) and loss factor (tanδ) of neat epoxy and hierarchical composites. Morphologies of fracture structures obtained after mechanical testing were characterized by SEM. Interfacial shear strength was investigated using single-fiber fragmentation test. During the testing, the condition of fiber fragmentation was monitored by polarized light microscope and the number of fiber fragments was counted within the gauge length of 14 mm. While, birefringence images of CF/EP-CNTs formed around the break points were unable to be received under polarizing microscope because the presence of CNTs in the resin led to the opaque of matrix. To solve this problem, we presented a novel method of single-fiber fragmentation test combined with EDS. Because of carbon element content of the fiber and matrix was differed considerably, the break points of CFs could emerge from EDS mapping scanning spectra. After the sample broken, the fracture cross-section was observed by SEM in order to evaluate the bond of the interface. To estimate the interfacial microstructures between carbon fiber and matrix, we used test techniques EDS (JEOL JSM-5900LV) equipped on SEM, f-AFM (CSPM 5500, China) and TEM.

3. Results and discussion

3.1. Performances of CFs

Surface topographies of virgin, unsized and deposited CFs were appraised by SEM and TEM (Fig. 4). Virgin CFs had smooth surface which could be seen at Fig. 4(a). During the production process, CFs were coated with a layer of sizing agent which gave carbon fiber a smooth surface. After removing the commercial sizing, the surfaces of CFs became smoother but with some grooves along the fibers,

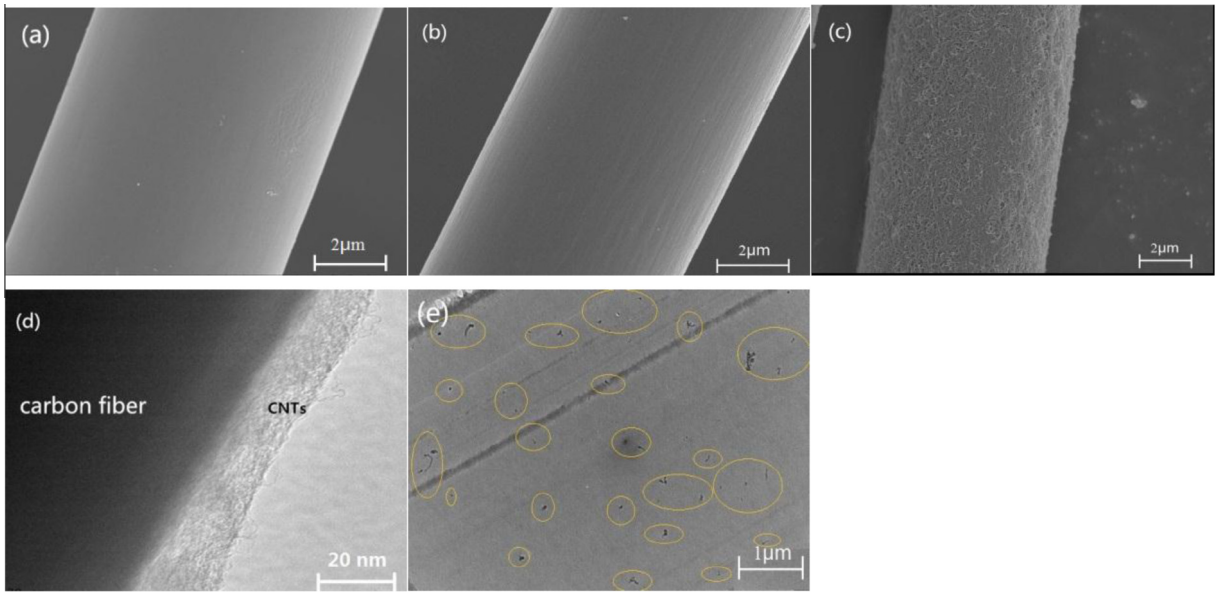

Fig. 4. Morphologies of CFs: (a) Virgin CFs; (b) CFs; (c) CF-CNTs; TEM images of (d) CF-CNTs and (e) modified matrix.

Table 1
Measured physical and mechanical properties of single fiber specimens.

Fiber type	Diameter (μm)	W. shape ρ	W. scale σ (MPa)	Modulus (GPa)	No. of samples
Virgin CFs	7.15	4.08	4920.46	281.5	26
CFs	6.67	3.64	4794.62	273.9	27
CF-CNTs	6.82	3.25	3980.6	264.6	27

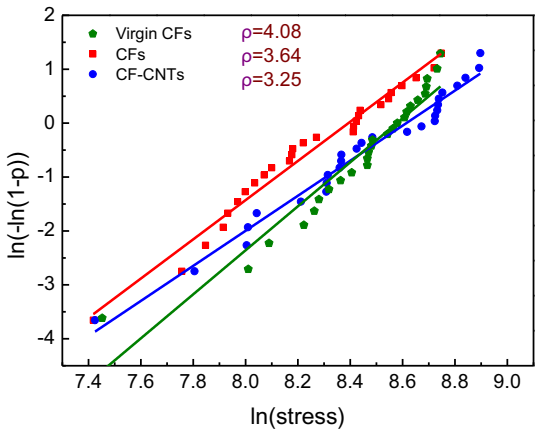

Fig. 5. Weibull plots of tensile treatments.

increasing carbon fiber specific area, as shown in Fig. 4(b). In Fig. 4(c) and (d), CNTs were successfully introduced onto CFs and well-distributed, which might heighten the bondings with matrices. Similarly, CNTs were homogeneously distributed in matrix with relatively meager content (Fig. 4(e)) compared with reference [31]. We believed that CNTs in resin might merely enhance the matrix instead of the interface between fiber and matrix.

The fiber tensile results, noted in Table 1, expressly demonstrated that the surface preparations played important roles in tensile properties of fibers. After desizing, fiber dimeter (6.67 μm) was lessened compared with virgin CFs (7.15 μm), however fiber diameter (6.82 μm) was slightly increased due to the deposition of CNTs. We can characterize the variability of the fiber tensile strength through Weibull shape parameters (ρ). The greater the value expresses the smaller dispersity of the strength, the less brittleness and the better toughness. The value of Weibull scale parameter (σ) was the measured mean tensile strength examined by tensile tests. As exhibited in Table 1, the removal of fiber sizing slightly decreased fiber tensile strength (lower Weibull scale parameter, 4794.62 MPa) and increased the fiber dispersity (lower Weibull shape parameter, 3.64) compared with virgin CFs. Deposited CFs were measured to have the lowest tensile modulus and strength out of all types measured, with modulus and strength values of 264.6 GPa and 3980.6 MPa, respectively, mild decreases of 3.4% in modulus and 16.98% in ultimate strength as compared to unsized CFs. While CFs were exposed to the electric field 5 min and undergone the drying progress, mild defects might be imported to the fiber surface despite carbon nanotubes were introduced on the carbon fiber surface thereby decreasing fiber strength. Compared with CVD and chemical grafting which bring about decreases in fiber tensile strength of around 15–55% [32–34], EPD process did not make a notable reduction in the tensile strength of carbon fiber.

3.2. Mechanical properties of hierarchical composites

Three-point short beam bending method was carried out and the results were shown in Fig. 6(b). We obtained 10.22 and 15.14% increases in flexural strength and flexural modulus, respectively, over the CF/EP, with the addition of CNTs to the epoxy matrix. The flexural strength of CF-CNTs/EP has been clearly enhanced by 18.43% and the flexural modulus was evidently improved by 27.01% with the addition of CNTs on CFs via EPD.

To better understand the role of CNTs, we investigated the tensile properties of composites and the results could be seen in Fig. 6(a). It was obviously attested that the tensile strength of composites containing CNTs was higher than that of CF/EP, indicating a similar enhancement trend to the flexural properties, and the tensile strength increased by 10.41 and 24.42% for CF/EP-CNTs and CF-CNTs/EP. The tensile properties of carbon fiber reinforced composites were in general dominated by the fiber behavior [16,35,36]. Due to the fact that the fiber types of CF/EP and CF/EP-CNTs were the same, the reason why the mild increase in tensile properties for CF/EP-CNTs was received may be that CNTs in CF/EP-CNTs just enhanced the toughness of the epoxy matrix. Moreover, numerous OCNTs in matrix could relieve major cracks and induce more microcracks when the major crack extended to them, which could absorb the fracture energy and delay the occurrence of damages [19,55]. But, in CF-CNTs/EP, a mild decrease of ultimate strength for CF-CNTs was obtained compared with unsized CFs. Therefore, the increase in tensile strength for composites cannot be attributed to the fiber behavior. In CF-CNTs/EP, CNTs in interface region strengthened the interphase which played a key

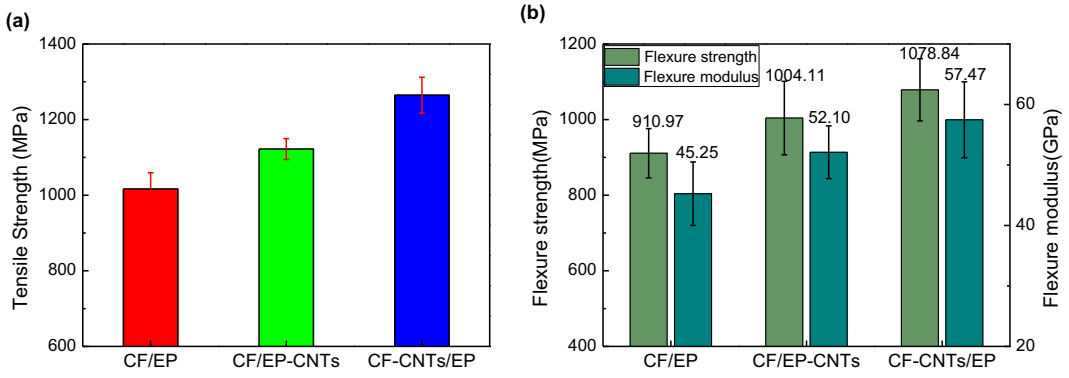

Fig. 6. Tensile and flexural performances of CF/EP, CF/EP-CNTs and CF-CNTs/EP.

part in debonding failure process. The interface might be significantly beneficial to decrease stress concentration, prevent the cracks to directly spread to the fiber surface, reduce debondings and pulling out and raise the tensile properties of composites [38,55].

3.3. Thermal properties of hierarchical composites

Dynamic mechanical thermal analysis can characterize the viscoelastic properties of the materials and be used to determine storage modulus (E′) and loss factor (tanδ) of neat epoxy and hierarchical composites [37–40]. The results indicated that the value of E' for hierarchical composites was far higher than that of the neat epoxy (4340 MPa). As revealed in Fig. 7(a), the value of E' improved from 4340 (EP) to 49,900 (CF/EP), 71,978 (CF/EP-CNTs) and 64,032 MPa (CF-CNTs/EP) below glass transition temperature (T_g). Meanwhile E' increased from 492 to 7853 (CF/EP), 9660 (CF/EP-CNTs), and 14,382 MPa (CF-CNTs/EP) when the temperature was above T_g respectively. The increases of E' indicated that the presences of CFs and CNTs substantially heightened the stiffness of composites at the whole temperature range. The reason may be that the stiffness of CFs was far greater than that of matrix (for CF/EP, CF/EP-CNTs and CF-CNTs/EP), CNTs strengthened the matrix when CNTs was mixed with resin (for CF/EP-CNTs) and the deposition of CNTs made a better interfacial adhesion between matrix and CFs, which can bring an increase in the volume fraction of interphase in the composites and a decrease in the effective polymer chain mobility at the interphase region [41]. This interphase area could work as an additional reinforcement for mechanical stiffening of the composites [16,42]. In the vicinity of the glass transition temperature, the mechanical loss of the polymer has a maximum value, which can help to determine T_g of the polymer. The temperature at which the loss factor curve showed a maximum peak was often used and recorded as the T_g [37–39]. We can see that, compared with neat epoxy (T_{gEP}, 128 °C), treatment of fiber or matrix only slightly improved T_g. Below $T_{gCF/EP\text{-}CNTs}$ (130 °C), CF/EP-CNTs had the biggest E' compared with neat epoxy and hierarchical composites, which showed that CF/EP-CNTs composites presented a superior heat-resistance property. However, when the temperature was above $T_{gCF\text{-}CNTs/EP}$ (133 °C) CF-CNTs/EP has a higher E' compared with CF/EP-CNTs which illustrated that the heat resistance of the former was better than that of the latter in the higher temperature range ($T_{gCF\text{-}CNTs/EP}$ to 200 °C). The loss factor curve of CF/EP-CNTs was the widest compared with neat epoxy and hierarchical composites which evinced that the length distribution range of molecular chain segments in the matrix was the widest. It may be due to the fact that carboxylic acid groups loaded on the CNTs and carbon fiber surface reacted with epoxy groups of resin which increased the length of molecular chain segments. The increase of T_g and decrease of tanδ for CF-CNTs/EP containing CNTs probably might be due to the enhancement of a restricted mobility interphase region composed of CNTs and epoxy [43].

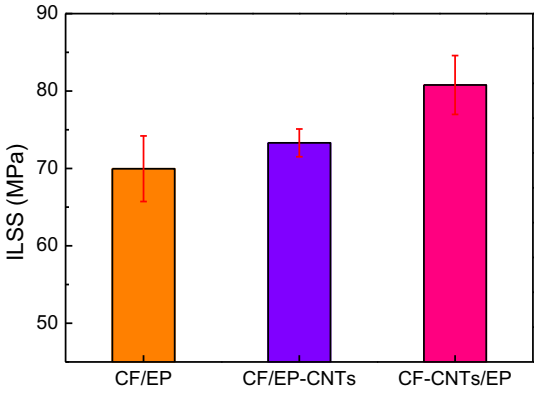

Fig. 8. Interlaminar shear strengthes of CF/EP, CF/EP-CNTs, and CF-CNTs/EP.

3.4. Interfacial properties of hierarchical composites

In order to roughly estimate and compare the interfacial bonding strength, the interlaminar shear strength, which differ from the microscopic mechanics testing method [44,45], has been implemented. In Fig. 8, a mild increase in the ILSS value (73.30 MPa) with an improvement of 4.77% compared with CF/EP was obtained owing to matrix modification. Another method for introducing CNTs into composites, interface modification (EPD), provided a good interfacial property and the ILSS value was 80.78 MPa with an obvious improvement of 15.47%.

More and more scholars are using single-fiber fragmentation test to characterize the interfacial properties of composites by analyzing IFSS of single fiber [30,46–48]. Fig. 9(a) provides a schematic of the single-fiber fragmentation test. The gauge length was divided by the fragments to determine average fragment length (l_{avg}), and saturation was achieved for all samples used in calculation. Single-fiber fragmentation test results for each type of carbon fiber combined with different matrices could be seen in Table 2.

The estimation of critical fiber length (l_c) calculated from the optical micrographs or EDS mapping scanning spectra of the fragmented specimens gave a qualitative characterization of the interphase between fiber and matrix, and the optical micrographs and EDS mapping scanning spectra were exhibited in Fig. 9. We can see that l_c of unsized CFs in neat epoxy matrix had the maximum

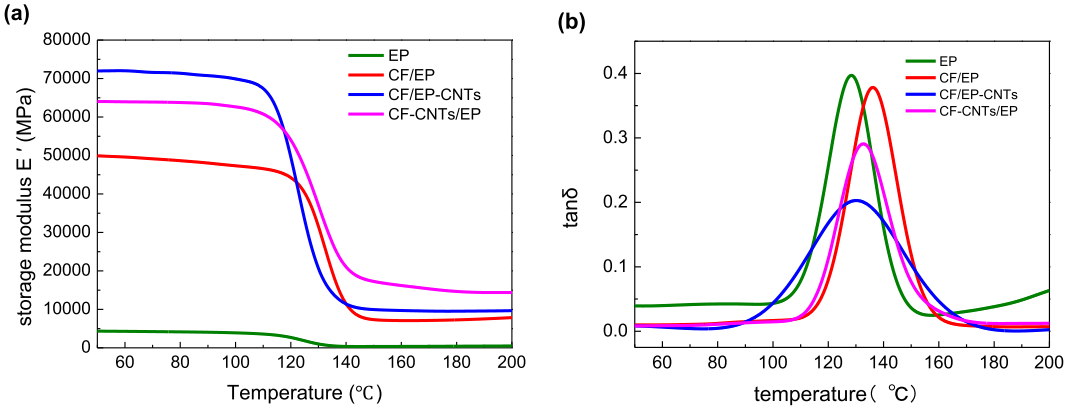

Fig. 7. DMA of epoxy and its composites: (a) storage modulus (E′) and (b) loss factor (tanδ).

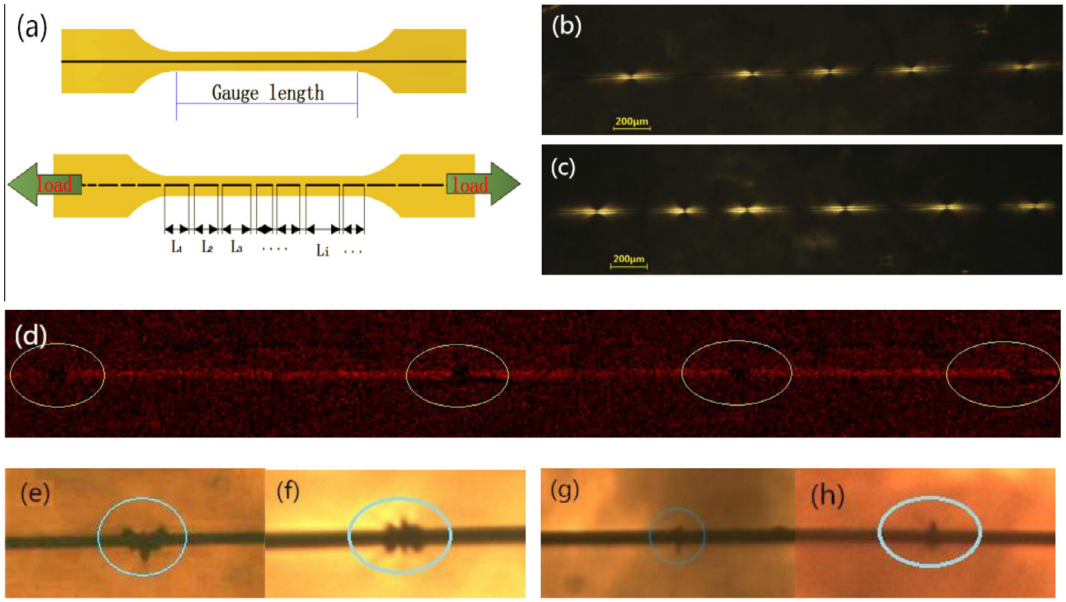

Fig. 9. Schematic of the fiber fragmentation test (a); birefringence effects of fragmented specimens: (b) CFs in EP matrix, (c) CF-CNTs in EP matrix; EDS mapping scanning spectra: (d) CFs in EP-CNTs matrix; micro-damage images of (e) and (f) CF-CNTs, (g) and (h) CFs.

Table 2
Single-fiber fragmentation test results for each type of carbon fiber combined with different matrices.

Fiber type (matrix)	Critical length l_c (μm)	σ_f (GPa)	W. scale σ (MPa)	W. shape ρ	IFSS (MPa)
CFs (EP)	746.7	10.07	4794.62	3.64	47.91
CFs (EP-CNTs)	666.7	10.55	4794.62	3.64	52.77
CF-CNTs (EP)	533.3	10.88	3980.60	3.25	69.56

value (746.7 μm); unsized CFs combined with CNT-reinforced matrix had the medium value (666.7 μm) and the deposited CFs in epoxy matrix have the minimum l_c (533.3 μm). Corresponding to l_c, the unsized CFs combined with neat epoxy presented the lowest IFSS (47.91 MPa) shown in Table 2. Compared with CF/EP, increases of 10.14% and 45.2% were achieved for CF/EP-CNTs and CF-CNTs/EP respectively. The calculated fiber strength (σ_f) at the critical length, to a certain extent, influenced the value of IFSS. Due to the values of σ_f for the two fiber types were extremely approximate, the increase of IFSS should be attributed to the strengthening of the interface between fiber and matrix. Although the interface was the weak part of fiber/matrix composite, but the efficiency of stress transmission between fiber and matrix, the recovery and distribution of stress on fracture fiber were decided by the interface performance, so that interface, in a great extent, effected the macroscopical mechanical properties [47].

The micro-damage phenomena generated after fiber break in single-fiber fragmentation tests was another significative factor influencing mechanical strength, depending on the interfacial adhesion. The micro-damage images of breaks were shown in Fig. 9. In contrast to the unsized CFs without deposition, breaks of deposited CFs were typically large and extended into the matrix. The interface of unsized single-fiber composite was relatively weak and the capacity of passing the stress to matrix was poor, so that damages were rarely expanded to the resin and debondings were preferential to happen. After the deposition of CNTs, the interface was strengthened by CNTs around carbon fiber. A sturdy interphase made the load distribute uniformly and transfer from fiber to the resin effectively when the single-fiber composite was damaged, resulting in fiber break and resin fracture were relatively large [47] and the birefringence phenomenon was especially obvious (Fig. 9(c)).

We next investigated fracture mechanism of the single-fiber composite and the cross-sections were characterized using SEM characterizations (Fig. 10). Due to the fact that unsized carbon fiber single-composite has a weak interface, carbon fiber was pulled out from the matrix completely and the resin fracture surface was very neat (Fig. 10(a)). CF/EP-CNTs with the medium interface in which debonding was occurred too but the adhesion between fiber and matrix was very strong for CF-CNTs/EP and the section neat without fiber pulled out and debonding (Fig. 10(c) and (d)).

3.5. Interfacial microstructure and enhancement mechanisms

After mechanical tests, fracture structures were obtained and the fracture morphologies were surveyed by SEM. In Fig. 11, there were the pictures of fracture surface which can help us understand the reinforcing mechanisms of CNTs introduced by two different methods. For the fracture surface of CF/EP (Fig. 11(a) and (b)), carbon fiber surface was very clean and the matrix was comparatively neat which indicated a weak interface resulting failure debonding between carbon fiber and matrix [49,50]. Compared with CF/EP, carbon fiber surface of CF/EP-CNTs (Fig. 11(c) and (d)) was sticky with some resin and the facture section was slightly rough. In Fig. 11(e) and (f), there was more resin adhering to the carbon fiber surface and we could notice that an amount of CNTs (marked in circles) were existed in interface region which indicated a strong interphase. From these images, it could be seen that interface modification played a key part in debonding failure process and a large part of fractures were occurred in interface area.

As stated in the preceding, significant improvements in mechanical properties, thermal properties and interfacial properties for CF-CNTs/EP were achieved compared to CF/EP and CF/EP-CNTs.

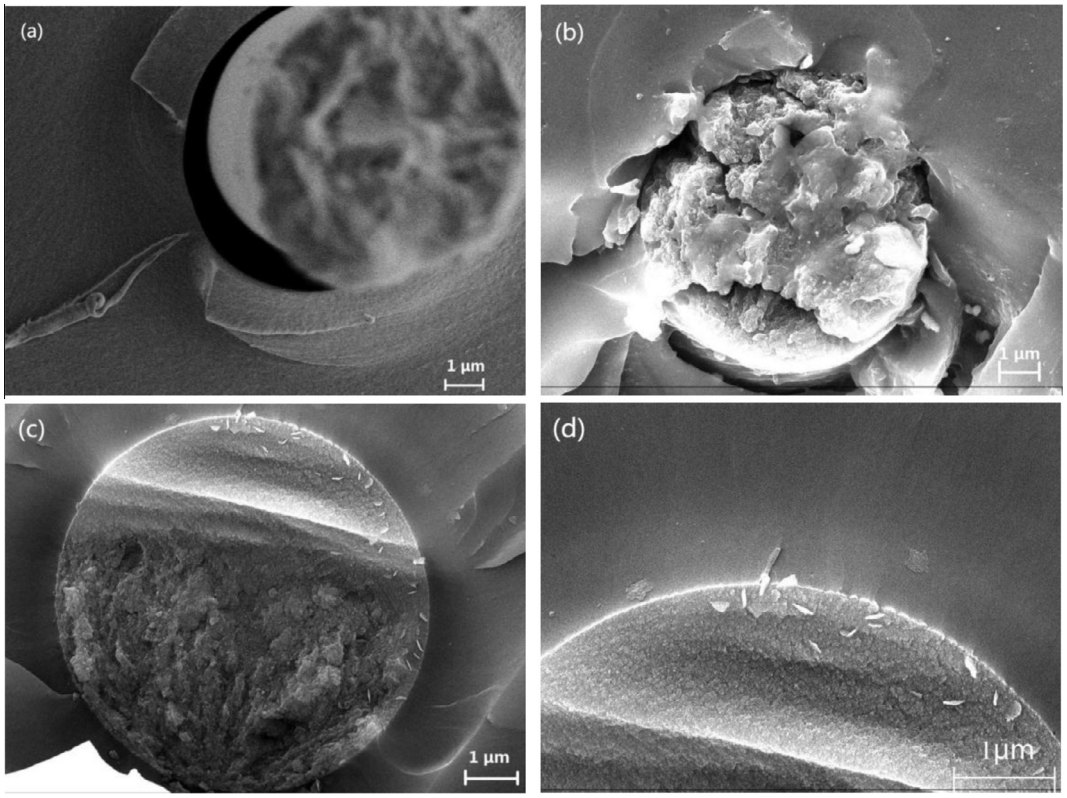

Fig. 10. SEM images for cross-sections of the single-fiber composites (a) CF/EP, (b) CF/EP-CNTs, (c) CF-CNTs/EP and (d) high resolution micrographs of (c).

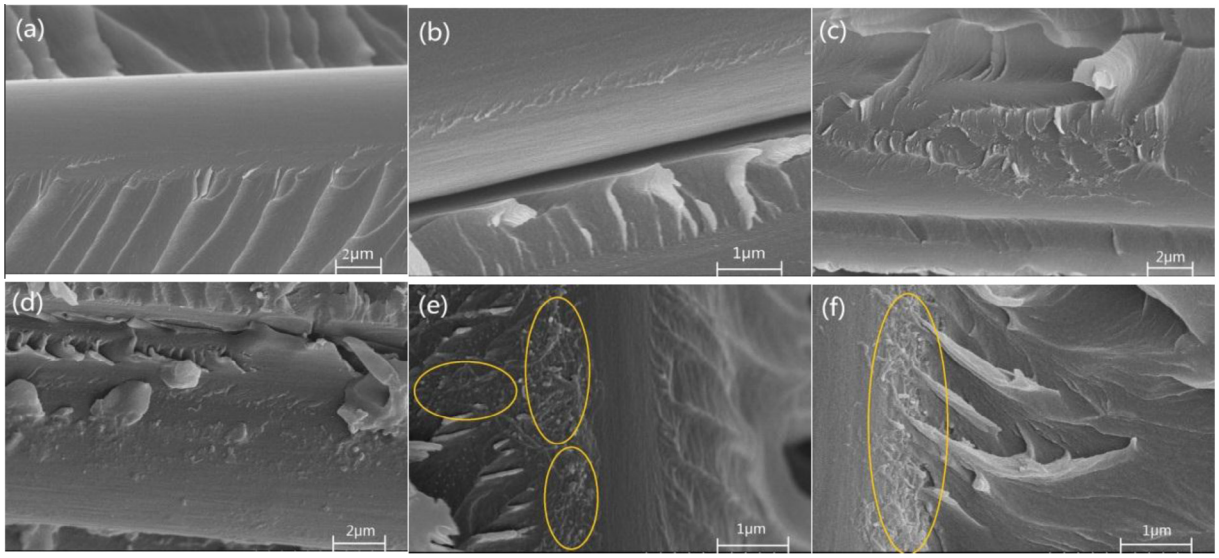

Fig. 11. Fracture surface of carbon fiber/epoxy composites: (a) and (b) CF/EP, (c) and (d) CF/EP-CNTs, (e) and (f) CF-CNTs/EP.

There have been some generally recognized strengthening mechanisms, which were proposed for explaining the interfacial improvements of fiber/polymer composites using CNTs [12,32,34,51–54]. These interfacial reinforcing mechanisms can be summarized as five aspects [30]: (1) Van der Waals binding due to increased specific surface area of fiber, (2) mechanical interlocking of CNTs with matrix, (3) surface wettability of fiber by polymer, (4) chemical bonding between CNTs and bulk materials including fiber and matrix, and (5) local stiffening or strengthening of polymer matrix near fiber/matrix interface.

According to the morphologies and roughness of the deposited carbon fiber surface (Fig. 5(c)), it can be believed that Van der Waals binding, increasing the interfacial friction and restricting the movement of the different phase of the materials at the composite interface [30], played roles in the interfacial improvement partly. Functional CNTs have many functional groups, which can react with the epoxy groups, making a better surface wettability of fiber by polymer and forming lots of micro interface. In addition, we present a novel enhancement mechanism which had been discussed in our previous paper [19,38,55]: during the progress

of composite molding, some CNTs dropped from deposited carbon fiber surface and dispersed into matrix while a gradient interface layer which has gradient properties between fillers and matrix might be formed. Due to the fact that the toughness of the epoxy matrix containing very low content of the functionalized CNTs increases significantly, so that the toughness, for the gradient interface layer, from fiber to matrix reduced gradually. Compared with chemical modification on carbon fiber surface [49], the chemical inertness and less reactive functional groups of CFs decided that there was scarcely any chemical bonding could be formed between CFs and CNTs. Furthermore, after electrophoretic deposition, the CNTs tended to lie in the plane of the carbon fiber surface. Thus, the deposited CNTs lying on fiber surface may not be contributed to increasing mechanical interlock between CNTs and matrix. While, grafting CNTs onto fiber surfaces via CVD [14,34] could provide CNTs with a radial orientation, which was expected to offer a strong mechanical interlocking interaction favoring transverse reinforcement. However, chemical methods [15,16] to covalently graft CNTs onto reinforcing fibers could provide firm combinations between functionalised CNTs and fibers, which was similar to CVD. CNTs, which were combined with reinforcing fibers firmly, will not drop from fiber surface and disperse into matrix during the progress of composite molding, which was contrary to deposited CNTs. Therefore, we deemed that the gradient interface layer theory was the primary enhancement mechanism and the gradient interface layer might be significantly beneficial to decrease stress concentration, effectively facilitated the stress transfer from the matrix to the reinforcements and raised the mechanical properties of composites.

In order to validate the existence of gradient interface layer, techniques of EDS equipped on SEM, f-AFM and TEM were employed and the results were presented in Figs. 12–14.

By scanning the distribution of carbon element [19,56] on the cross-section of composites, the microstructure of the interface-phase was confirmed. For CF/EP, the contour profile of the carbon fiber was clear (Fig. 12(a)) and a sudden decrease in the content of carbon element along the yellow line was shown in Fig. 12(d), illustrating that carbon content of the fiber and matrix was differed considerably. It can be foreseen that the results, for CF/EP-CNTs, of EDS mapping scanning spectra were similar to that of CF/EP. The outline of carbon fiber was obvious too and the interphase thickness value (0.84 μm) calculated from the line scanning result was close to CF/EP (0.65 μm). Whereas in the cross-section of CF-CNTs/EP, it was hard to distinguish boundary between carbon fiber and matrix, indicating the presence of CNTs in interface. Corresponding to Fig. 12(c), carbon element content decreased gradually from fibers to matrix (shown in Fig. 12(f)) and the interphase thickness value (1.34 μm) was the biggest compared with CF/EP and CF/EP-CNTs, which demonstrated the gradient distribution of CNTs in the interface layer.

The cantilever tip of AFM indenting into the sample surface gives a description about the local modulus of sample surface [19]. On the stiff areas of the sample surface, the deflection of cantilever was smaller, and on the soft areas larger. The relative stiffness value will be indirectly indicated by the voltage generated from the cantilever deflection [57,58]. The force modulation images and illustrations of stiffness distribution along the dotted line in corresponding images obtained from the cross-section of the composites were shown in Fig. 13. As illustrated in Fig. 13, the interphase thickness values for CF/EP, CF/EP-CNTs and CF-CNTs/EP were 437, 478 and 1288 nm respectively which were basically consistent with the EDS linear scanning results and the slight difference might be due to the difference of test methods or disparity of samples. Therefore, the existence of gradient interface layer was authenticated from another point of view by detection of the modulus distribution in composite cross-section.

In order to observe the existence of gradient interface layer more directly, we surveyed the ultrathin section of composites (Fig. 14). Because the procedure for preparation of the thin foils for TEM was highly complex [3,59], we selected the conductive nylon fibers to replace CFs owing to the fiber type will not affect the diffusion of CNTs. From TEM images, gradient distribution of CNTs can be observed in the direction of the fiber surface to the matrix and the interface-phase had a certain thickness.

In virtue of the explorations above we can conclude that, in CF-CNTs/EP, partial CNTs could diffuse into the matrix around

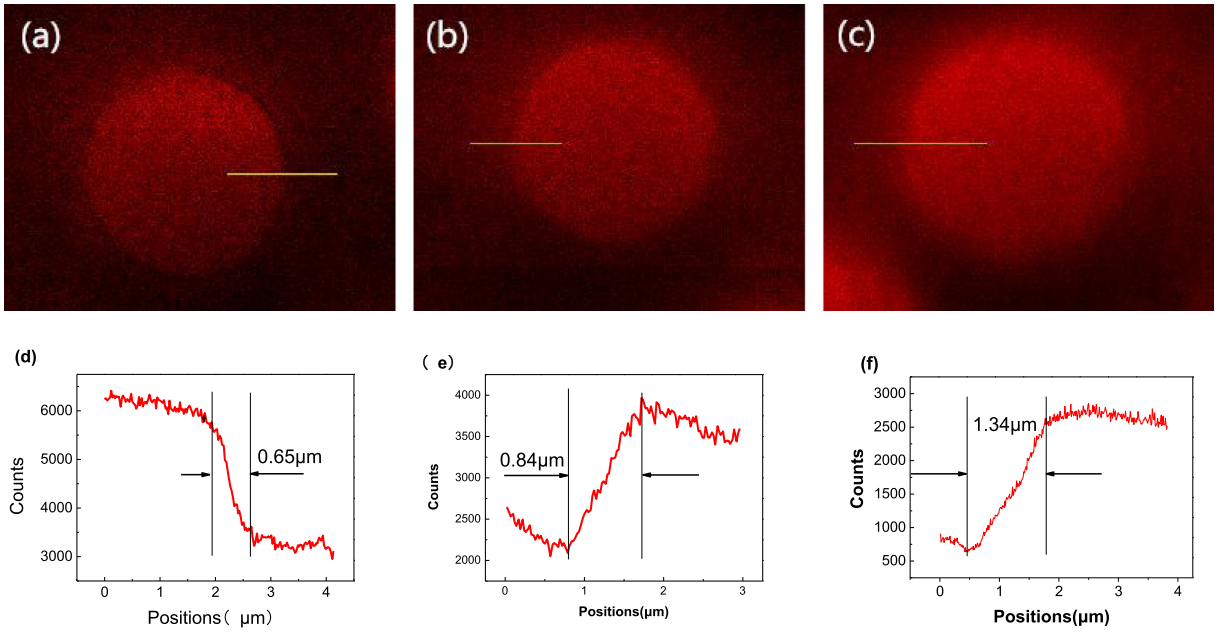

Fig. 12. Distribution of carbon element of composite cross-section (measured by EDS mapping scanning spectra): (a) CF/EP, (b) CF/EP-CNTs, (c) CF-CNTs/EP; distribution of carbon element (measured by EDS linear scanning system) along the yellow line: (d) CF/EP, (e) CF/EP-CNTs, (f) CF-CNTs/EP. (For interpretation of the references to color in this figure legend, the reader is referred to the web version of this article.)

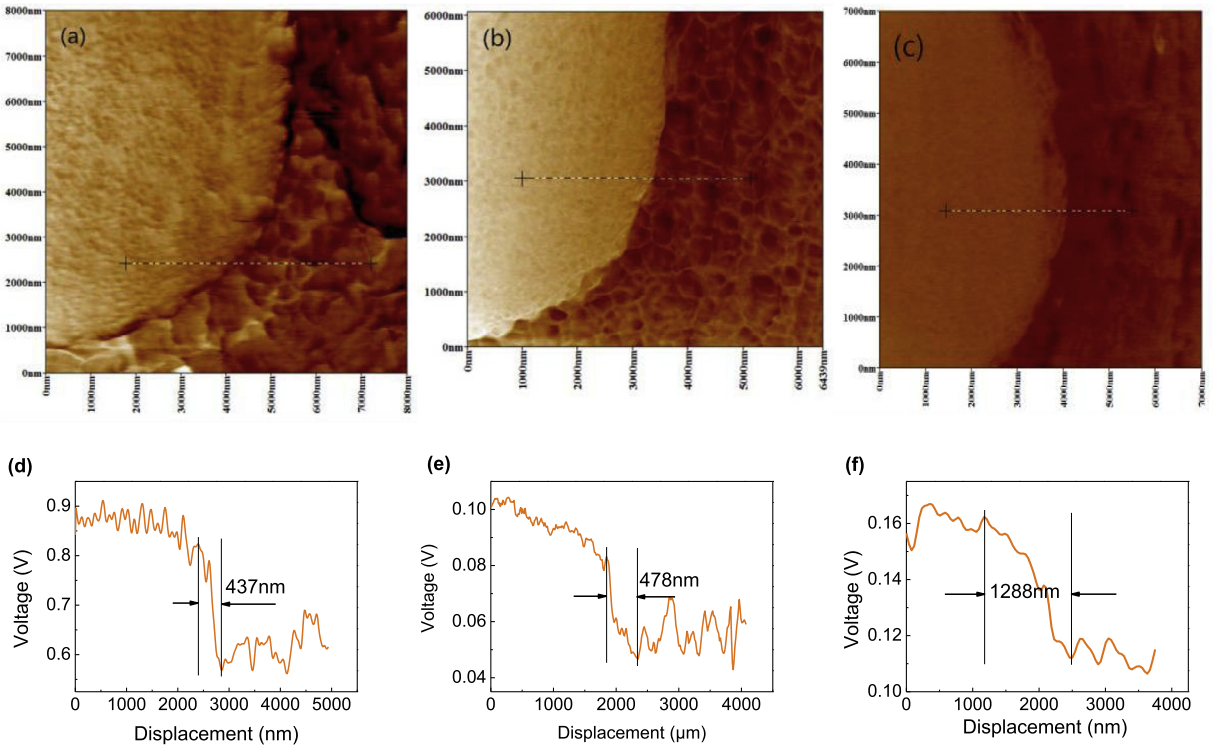

Fig. 13. Relative stiffness images and illustrations of stiffness distribution along the dotted line of cross-sections for (a and d) CF/EP, (b and e) CF/EP-CNTs, and (c and f) CF-CNTs/EP.

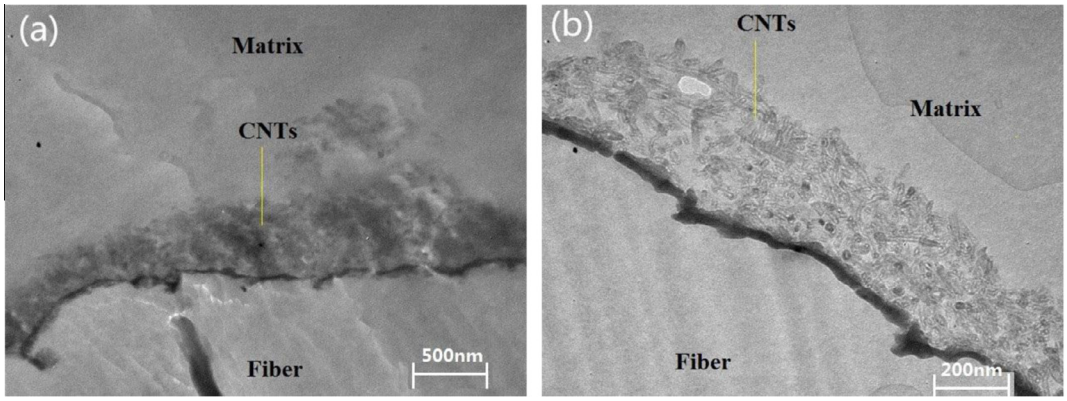

Fig. 14. TEM images of ultrathin section for deposited fiber.

the CFs during molding, which could tough the matrix and create a gradient interphase which could significantly beneficial to decrease stress concentration, effectively facilitate the stress transfer from the matrix to the reinforcements and ameliorate the composite performances. For CF/EP-CNTs, the mixture of resin and equivalent CNTs were merely toughened the matrix but the interface layer and the interface transition layer was absenced which indicate that the improvements of properties was greatly depended on the improvement of the properties of the matrix.

4. Conclusions

In this work, we obtained hierarchical composites based on CNT-reinforced matrix or CNT-modified fibers where CNTs were introduced via two substitutable routes: mixing CNTs entirely throughout the matrix or attaching CNTs directly onto reinforcing fibers where EPD was selected as a representative. CNTs were successfully introduced onto CFs and the CNT homogeneous distribution in matrix was authenticated by SEM and TEM. The following conclusions were summarized on account of systematic investigations and comparisons of matrix modification and interface modification:

1. We presented a novel method, single-fiber fragmentation test combined with EDS mapping scanning, to calculate IFSS of composites based on CNT-reinforced matrix. This technology could be employed to measure IFSS of composites with opaque matrix in which birefringence images formed around the break points were unable to be obtained under polarizing microscope.
2. Compared with CF/EP, increases of 10.41 (tensile strength), 10.22 (flexural strength) and 15.14% (flexural modulus) for CF/EP-CNTs, and improvements of 24.42 (tensile strength) 18.43 (flexural strength) and 27.01% (flexural modulus) for CF-CNTs/EP were obtained.

3. The introduction of CNTs increased the E′ of the composites. CF/EP-CNTs presented better heat-resistance property below T_g and worse heat-resistance property above T_g compared with CF-CNTs/EP. And $T_{gCF\text{-}CNTs/EP}$ (133 °C) was slightly higher than $T_{gCF/EP\text{-}CNTs}$ (130 °C).
4. CF-CNTs/EP showed a better interfacial performance than CF/EP-CNTs that increases of 15.47 (ILSS) and 45.2% (IFSS) for CF-CNTs/EP, and increases of 4.77% (ILSS) and 10.14% (IFSS) for CF/EP-CNTs compared with CF/EP were gained.
5. Explored by EDS, f-AFM and TEM, gradient interface layer between CFs and matrix, which could be significantly beneficial to decrease stress concentration, effectively facilitate the stress transfer from the matrix to reinforcements and raise the ultimate performance of composites, was formed in CF-CNTs/EP and it was not obvious in CF/EP-CNTs.
6. The approach of matrix modification generally has the advantages of simplicity and compatibility with standard industrial techniques and a strong interfacial bonding between the functionalized CNTs and matrix was acquired instead of a strong interface between fiber and matrix. However, interface modification providing the excellent mechanical properties and interfacial properties has a great advantage over matrix modification in fiber-reinforced polymer composites although the partial thermal performance of CF-CNTs/EP was worse than that of CF/EP-CNTs.

Acknowledgments

The work was funded by the Petrochemical Joint Fund of National Natural Science Fund Committee – China National Petroleum Corporation (U1362108), the National Natural Science Foundation of China (11575126) and the Natural Science Foundation of Tianjin (16JCZDJC37800, 15JCQNJC42400).

Appendix A. Supplementary data

Supplementary data associated with this article can be found, in the online version, at http://dx.doi.org/10.1016/j.compstruct.2016.10.022.

References

[1] Wu G, Ma L, Liu L, Wang Y, Huang Y. Interfacial improvement of carbon fiber-reinforced methylphenylsilicone resin composites with sizing agent containing functionalized carbon nanotubes. J Adhes Sci Technol 2015;29(21):2295–310.
[2] Godara A, Gorbatikh L, Kalinka G, Warrier A, Rochez O, Mezzo L, et al. Interfacial shear strength of a glass fiber/epoxy bonding in composites modified with carbon nanotubes. Compos Sci Technol 2010;70(9):1346–52.
[3] Tzounis L, Kirsten M, Simon F, Mäder E, Stamm M. The interphase microstructure and electrical properties of glass fibers covalently and non-covalently bonded with multiwall carbon nanotubes. Carbon 2014;73:310–24.
[4] Chou T-W, Gao L, Thostenson ET, Zhang Z, Byun J-H. An assessment of the science and technology of carbon nanotube-based fibers and composites. Compos Sci Technol 2010;70(1):1–19.
[5] Qian H, Greenhalgh ES, Shaffer MSP, Bismarck A. Carbon nanotube-based hierarchical composites: a review. J Mater Chem 2010;20(23):4751.
[6] CA. PMNMB. Mechanical, surface and interfacial characterisation of pitch and PAN-based carbon fibres. Carbon 2000;38(9):1323–37.
[7] Dvir H, Jopp J, Gottlieb M. Estimation of polymer-surface interfacial interaction strength by a contact AFM technique. J Colloid Interf Sci 2006;304(1):58–66.
[8] Park S-J, Kim B-J. Roles of acidic functional groups of carbon fiber surfaces in enhancing interfacial adhesion behavior. Mater Sci Eng A-Struct 2005;408(1–2):269–73.
[9] Fan Z, Hsiao K-T, Advani SG. Experimental investigation of dispersion during flow of multi-walled carbon nanotube/polymer suspension in fibrous porous media. Carbon 2004;42(4):871–6.
[10] Thostenson ET, Ziaee S, Chou T-W. Processing and electrical properties of carbon nanotube/vinyl ester nanocomposites. Compos Sci Technol 2009;69(6):801–4.
[11] Gojny FH, Wichmann MHG, Fiedler B, Bauhofer W, Schulte K. Influence of nano-modification on the mechanical and electrical properties of conventional fibre-reinforced composites. Compos Part A – Appl Sci Manuf 2005;36(11):1525–35.
[12] Thostenson ET, Li WZ, Wang DZ, Ren ZF, Chou TW. Carbon nanotube/carbon fiber hybrid multiscale composites. J Appl Phys 2002;91(9):6034.
[13] Jo SH, Wang DZ, Huang JY, Li WZ, Kempa K, Ren ZF. Field emission of carbon nanotubes grown on carbon cloth. Appl Phys Lett 2004;85(5):810.
[14] Yamamoto N, John Hart A, Garcia EJ, Wicks SS, Duong HM, Slocum AH, et al. High-yield growth and morphology control of aligned carbon nanotubes on ceramic fibers for multifunctional enhancement of structural composites. Carbon 2009;47(3):551–60.
[15] He X, Zhang F, Wang R, Liu W. Preparation of a carbon nanotube/carbon fiber multi-scale reinforcement by grafting multi-walled carbon nanotubes onto the fibers. Carbon 2007;45(13):2559–63.
[16] Zhao F, Huang Y, Liu L, Bai Y, Xu L. Formation of a carbon fiber/polyhedral oligomeric silsesquioxane/carbon nanotube hybrid reinforcement and its effect on the interfacial properties of carbon fiber/epoxy composites. Carbon 2011;49(8):2624–32.
[17] Mei L, Li Y, Wang R, Wang C, Peng Q, He X. Multiscale carbon nanotube-carbon fiber reinforcement for advanced epoxy composites. Polym Polym Compos 2011;19(2–3):107–12.
[18] Barber AH, Zhao Q, Wagner HD, Baillie CA. Characterization of E-glass–polypropylene interfaces using carbon nanotubes as strain sensors. Compos Sci Technol 2004;64(13–14):1915–9.
[19] Yao H, Sui X, Zhao Z, Xu Z, Chen L, Deng H, et al. Optimization of interfacial microstructure and mechanical properties of carbon fiber/epoxy composites via carbon nanotube sizing. Appl Surf Sci 2015;347:583–90.
[20] Wang J, Yin G, Chen Y, Li R, Sun X. Pd nanoparticles deposited on vertically aligned carbon nanotubes grown on carbon paper for formic acid oxidation. Int J Hydrogen Energy 2009;34(19):8270–5.
[21] Qian H, Bismarck A, Greenhalgh ES, Shaffer MSP. Synthesis and characterisation of carbon nanotubes grown on silica fibres by injection CVD. Carbon 2010;48(1):277–86.
[22] Laachachi A, Vivet A, Nouet G, Ben Doudou B, Poilâne C, Chen J, et al. A chemical method to graft carbon nanotubes onto a carbon fiber. Mater Lett 2008;62(3):394–7.
[23] Siddiqui NA, Sham M-L, Tang BZ, Munir A, Kim J-K. Tensile strength of glass fibres with carbon nanotube–epoxy nanocomposite coating. Compos Part A – Appl Sci Manuf 2009;40(10):1606–14.
[24] Jiang B, Huang YD. Quality inspection of laid fabric epoxy resins prepreg by near infrared spectroscopy. Compos Part A – Appl Sci Manuf 2008;39(5):712–7.
[25] Gao CJY, Kong H, Whitby RLD, Acquah SFA, Chen GY, et al. Polyurea-functionalized multiwalled carbon nanotubes: synthesis, morphology, and Raman spectroscopy. J Phys Chem B 2005;109:11925–32.
[26] Sharma M, Gao S, Mäder E, Sharma H, Wei LY, Bijwe J. Carbon fiber surfaces and composite interphases. Compos Sci Technol 2014;102:35–50.
[27] Zhou G, Byun J-H, Wang Y-Q, Cha H-J, Lee J-U, Jung B-M, et al. Mechanism of sonication-assisted electrophoretic deposition of carbon nano-fiber on carbon fabrics. Compos Sci Technol 2015;107:29–35.
[28] Moaseri E, Karimi M, Maghrebi M, Baniadam M. Fabrication of multi-walled carbon nanotube–carbon fiber hybrid material via electrophoretic deposition followed by pyrolysis process. Compos Part A – Appl Sci Manuf 2014;60:8–14.
[29] Li K-Z, Li L, Li H-J, Song Q, Lu J-H, Fu Q-G. Electrophoretic deposition of carbon nanotubes onto carbon fiber felt for production of carbon/carbon composites with improved mechanical and thermal properties. Vacuum 2014;104:105–10.
[30] Li M, Gu Y, Liu Y, Li Y, Zhang Z. Interfacial improvement of carbon fiber/epoxy composites using a simple process for depositing commercially functionalized carbon nanotubes on the fibers. Carbon 2013;52:109–21.
[31] Pötschke P, Bhattacharyya AR, Janke A. Carbon nanotube-filled polycarbonate composites produced by melt mixing and their use in blends with polyethylene. Carbon 2004;42(5–6):965–9.
[32] Qian H, Bismarck A, Greenhalgh ES, Shaffer MSP. Carbon nanotube grafted carbon fibres: a study of wetting and fibre fragmentation. Compos Part A – Appl Sci Manuf 2010;41(9):1107–14.
[33] Zhang Q, Liu J, Sager R, Dai L, Baur J. Hierarchical composites of carbon nanotubes on carbon fiber: influence of growth condition on fiber tensile properties. Compos Sci Technol 2009;69(5):594–601.
[34] Sager RJ, Klein PJ, Lagoudas DC, Zhang Q, Liu J, Dai L, et al. Effect of carbon nanotubes on the interfacial shear strength of T650 carbon fiber in an epoxy matrix. Compos Sci Technol 2009;69(7–8):898–904.
[35] Zhang X, Fan X, Yan C, Li H, Zhu Y, Li X, et al. Interfacial microstructure and properties of carbon fiber composites modified with graphene oxide. ACS Appl Mater Inter 2012;4(3):1543–52.
[36] Godara A, Mezzo L, Luizi F, Warrier A, Lomov SV, van Vuure AW, et al. Influence of carbon nanotube reinforcement on the processing and the mechanical behaviour of carbon fiber/epoxy composites. Carbon 2009;47(12):2914–23.
[37] Wan Y-J, Gong L-X, Tang L-C, Wu L-B, Jiang J-X. Mechanical properties of epoxy composites filled with silane-functionalized graphene oxide. Compos Part A – Appl Sci Manuf 2014;64:79–89.
[38] Chen L, Jin H, Xu Z, Shan M, Tian X, Yang C, et al. A design of gradient interphase reinforced by silanized graphene oxide and its effect on carbon fiber/epoxy interface. Mater Chem Phys 2014;145(1–2):186–96.
[39] Ni Y, Chen L, Teng K, Shi J, Qian X, Xu Z, et al. Superior mechanical properties of epoxy composites reinforced by 3D interconnected graphene skeleton. ACS Appl Mater Inter 2015;7(21):11583–91.

[40] Guan L-Z, Gong L-X, Tang L-C, Wu L-B, Jiang J-X, Lai G-Q. Mechanical properties and fracture behaviors of epoxy composites with phase-separation formed liquid rubber and preformed powdered rubber nanoparticles: a comparative study. Polym Compos 2015;36(5):785–99.
[41] Rahman MM, Zainuddin S, Hosur MV, Malone JE, Salam MBA, Kumar A, et al. Improvements in mechanical and thermo-mechanical properties of e-glass/epoxy composites using amino functionalized MWCNTs. Compos Struct 2012;94(8):2397–406.
[42] Eitan A, Fisher FT, Andrews R, Brinson LC, Schadler LS. Reinforcement mechanisms in MWCNT-filled polycarbonate. Compos Sci Technol 2006;66(9):1162–73.
[43] Martin-Gallego M, Hernández M, Lorenzo V, Verdejo R, Lopez-Manchado MA, Sangermano M. Cationic photocured epoxy nanocomposites filled with different carbon fillers. Polymer 2012;53(9):1831–8.
[44] Xu Z, Huang Y, Liu L, Zhang C, Long J, He J, et al. Surface characteristics of kidney and circular section carbon fibers and mechanical behavior of composites. Mater Chem Phys 2007;106(1):16–21.
[45] Xu Z, Li J, Wu X, Huang Y, Chen L, Zhang G. Effect of kidney-type and circular cross sections on carbon fiber surface and composite interface. Compos Part A – Appl Sci Manuf 2008;39(2):301–7.
[46] Schaefer JD, Guzman ME, Lim C-S, Rodriguez AJ, Minaie B. Influence of functionalized carbon nanofibers on the single carbon fiber–epoxy matrix interface. Compos Part B Eng 2013;55:41–7.
[47] Zhao FM, Takeda N. Effect of interfacial adhesion and statistical fiber strength on tensile strength of unidirectional glass fiber/epoxy composites. Part I: experiment results. Compos Part A – Appl Sci Manuf 2000;31(11):1203–14.
[48] Schaefer JD, Rodriguez AJ, Guzman ME, Lim C-S, Minaie B. Effects of electrophoretically deposited carbon nanofibers on the interface of single carbon fibers embedded in epoxy matrix. Carbon 2011;49(8):2750–9.
[49] Xu Z, Wu X, Sun Y, Jiao Y, Li J, Chen L, et al. Surface modification of carbon fiber by redox-induced graft polymerization of acrylic acid. J Appl Polym Sci 2008;108(3):1887–92.
[50] Xu Z, Huang Y, Zhang C, Liu L, Zhang Y, Wang L. Effect of γ-ray irradiation grafting on the carbon fibers and interfacial adhesion of epoxy composites. Compos Sci Technol 2007;67(15–16):3261–70.
[51] An F, Lu C, Li Y, Guo J, Lu X, Lu H, et al. Preparation and characterization of carbon nanotube-hybridized carbon fiber to reinforce epoxy composite. Mater Des 2012;33:197–202.
[52] Davis DC, Wilkerson JW, Zhu J, Hadjiev VG. A strategy for improving mechanical properties of a fiber reinforced epoxy composite using functionalized carbon nanotubes. Compos Sci Technol 2011;71(8):1089–97.
[53] Mei L, Li Y, Wang R, Wang C, Peng Q, He X. Multiscale carbon nanotube-carbon fiber reinforcement for advanced epoxy composites with high interfacial strength. Polym Polym Compos 2011;19(2–3):107–12.
[54] Zhang F-H, Wang R-G, He X-D, Wang C, Ren L-N. Interfacial shearing strength and reinforcing mechanisms of an epoxy composite reinforced using a carbon nanotube/carbon fiber hybrid. J Mater Sci 2009;44(13):3574–7.
[55] Chen L, Jin H, Xu Z, Li J, Guo Q, Shan M, et al. Role of a gradient interface layer in interfacial enhancement of carbon fiber/epoxy hierarchical composites. J Mater Sci 2014;50(1):112–21.
[56] Jiang B, Liu W, Bai Y, Huang Y, Liu L, Han J. Preparation and microcosmic structural analysis of recording coating on inkjet printing media. Int J Mol Sci 2011;12(8):5422–7.
[57] Munz M, Sturm H, Schulz E, Hinrichsen G. The scanning force microscope as a tool for the detection of local mechanical properties within the interphase of fibre reinforced polymers. Compos Part A – Appl Sci Manuf 1998;29(9–10):1251–9.
[58] Mai K, Mäder E, Muhle M. Interphase characterization in composites with new non-destructive methods. Compos Part A - Appl Sci Manuf 1998;29(9–10):1111–9.
[59] Zhou G, Liu Y, He L, Guo Q, Ye H. Microstructure difference between core and skin of T700 carbon fibers in heat-treated carbon/carbon composites. Carbon 2011;49(9):2883–92.